

Your thesaurus codes are:
06(02.08.1,02.20.1,08.13.1,08.16.5,08.18.1)

Magnetic field generation in weak-line T Tauri stars: An α^2 -dynamo

M. Küker and G. Rüdiger

Astrophysikalisches Institut Potsdam, An der Sternwarte 16, D-14482 Potsdam, Germany

Received date; accepted date

Abstract. We present a model for the generation of magnetic fields in fully convective pre-main sequence stars. The dynamo process in this type of star is of α^2 -type and hence quite different from the solar dynamo. Based on a mean field model of the turbulent electromotive force, the nonlinear induction equation is solved in three dimensions to allow for non-axisymmetric solutions. The resulting magnetic field is purely non-axisymmetric and steady.

Key words: Hydrodynamics – Turbulence – Stars: magnetic fields – Stars: pre-main sequence – Stars: rotation

1. Introduction

Magnetic fields play an essential role in stellar angular momentum evolution because the only way to extract angular momentum from a single star is magnetic coupling to the surrounding gas. This mechanism is particularly important in classical T Tauri systems (CTTS), where the stellar magnetic fields may thread the surrounding protoplanetary accretion disks.

In this type of system, the magnetic field prevents disk accretion inside the corotation radius and forces the gas to flow along the field lines towards the poles of the star (Camenzind 1990; Königl 1991; Shu et al. 1994). Outside the corotation radius, the disk is threaded by the field which exerts a positive torque on the disk, i.e. transfers angular momentum from the star to the disk and regulates the stellar rotation (Bouvier et al. 1993; Cameron & Campbell 1993; Edwards et al. 1993; Yi 1994; Ghosh 1995; Armitage & Clarke 1996; Li et al. 1996).

In the papers listed above, a dipolar magnetic field has been assumed with the axis of the dipole aligned with the axis of rotation. As long as the true field geometry is unknown, this assumption is the most reasonable one. As the efficiency of the disk braking mechanism strongly depends on the structure and strength of the stellar magnetic field (Wang 1995), this assumption must, however, be checked. Spot distributions obtained by Doppler imaging show non-axisymmetric patterns with large polar spots (Joncour et al. 1994a, 1994b; Hatzes 1995; Rice

& Strassmeier 1996; Johns-Krull & Hatzes 1997) and do not support the assumption of an aligned dipole.

While the magnetic field of a CTTS is influenced by the presence of the disk, that of a weak-line T Tauri star (WTTS) is completely determined by the properties of the star. As T Tauri stars are fully convective (at least during the early T Tauri phase), a fossil field can be excluded. It would not survive longer than a few hundred years because the convective motions enhance the efficiency of Ohmic dissipation for large-scale fields by about ten orders of magnitude. The field must be the result of a dynamo. Due to the lack of both differential rotation and a radiative core, it must be expected to be quite different from the solar dynamo (Küker & Rüdiger 1997). The most likely process is an α^2 -dynamo, which is known to produce non-axisymmetric fields under certain conditions (Rüdiger & Elstner 1994).

2. The dynamo

It is now widely accepted that the solar dynamo operates in the overshoot layer at the bottom of the convection zone, where the stratification of the turbulence dominates and the radial gradient of the angular velocity is positive. The resulting dynamo is of $\alpha\Omega$ -type with an oscillating field and equatorwards moving field belts in the equatorial region as required by the solar butterfly diagram (Krause & Rädler 1980; Schüssler 1983; Parker 1993).

While this model is quite successful in explaining the solar activity cycle, it can not be applied to fully convective stars. Observations as well as theoretical considerations lead to the conclusion that T Tauri stars rotate almost rigidly (Küker & Rüdiger 1997). A dynamo is of $\alpha\Omega$ -type if the rotational shear is more effective than the α -effect, i.e.

$$C_{\Omega} \gg C_{\alpha}, \quad (1)$$

where $C_{\Omega} = \alpha R^2 / \eta_T$ and $C_{\alpha} = R^3 \Omega / \eta_T$ are the magnetic Reynolds numbers corresponding to the two field generating processes, Ω is the angular velocity of the stellar rotation and R is a characteristic length scale, e.g. the stellar radius. In T Tauri stars, the absence of an overshoot layer as well as the flat rotation profile make a pure $\alpha\Omega$ -mechanism unlikely. Moreover,

the α -effect due to density stratification can not be ignored any longer but must be expected to be the dominating part of the α -effect.

2.1. The electromotive force

We work within the framework of mean field magnetohydrodynamics. In this approach, quantities are split into a large-scale and a small-scale part by application of an appropriate averaging procedure. We write as usual

$$\mathbf{B} = \langle \mathbf{B} \rangle + \mathbf{B}', \quad \mathbf{u} = \langle \mathbf{u} \rangle + \mathbf{u}'. \quad (2)$$

The induction equation for the mean magnetic field then reads

$$\frac{\partial \langle \mathbf{B} \rangle}{\partial t} = \nabla \times (\langle \mathbf{u} \rangle \times \langle \mathbf{B} \rangle + \mathcal{E}), \quad (3)$$

where $\mathcal{E} = \langle \mathbf{u}' \times \mathbf{B}' \rangle$ is the electromotive force (EMF) due to turbulent convection. It consists of a field generating and a diffusive term, i.e.

$$\mathcal{E}_i = \alpha_{ij} \langle B_j \rangle + \eta_{ijk} \frac{\partial \langle B_j \rangle}{\partial x_k}. \quad (4)$$

2.1.1. α -effect

While the eddy diffusivity η_T exists even in isotropic homogeneous turbulence, the α -effect is present only if the turbulent medium is stratified *and* rotates, i.e. the turbulence is neither homogeneous nor isotropic. In a rotating stellar convection zone, both density and the intensity of the turbulent motions, $u_t = \sqrt{\langle \mathbf{u}'^2 \rangle}$, are stratified. There are therefore two contributions to the α -effect, i.e.

$$\alpha = \alpha^\rho + \alpha^u. \quad (5)$$

In stellar convection zones, the density increases with depth while u_t decreases. Hence, the contributions to the total α -effect have different signs hence the final sign might vary with depth. In case of the Sun, the contribution from density dominates everywhere except in the transition layer at the bottom of the convection zone where the sign of α changes (Krivodubskij & Schultz 1993).

The α -effect due to the stratification of the convective motions runs with $\mathbf{U} = \nabla \log u_t$. As Fig. 1 shows, the convection velocity is constant throughout the star, α^u therefore vanishes and will not be considered any further. The contribution from density stratification is

$$\alpha_{ij}^\rho = -\delta_{ij} (\mathbf{\Omega} \mathbf{G}) \alpha_1^\rho - (\Omega_j G_i + \Omega_i G_j) \alpha_2^\rho - (\Omega_j G_i - \Omega_i G_j) \alpha_3^\rho - \frac{\Omega_i \Omega_j}{\Omega^2} (\mathbf{\Omega} \mathbf{G}) \alpha_4^\rho, \quad (6)$$

but $\mathbf{G} = \nabla \log \rho$ does not vanish and α^ρ is the field-generating term in the EMF.

Rewritten in cylindrical polar coordinates (s, ϕ, z) , the α -tensor reads

$$\alpha^\rho = \Omega^* G \tau_{\text{corr}} u_t^2 \cdot \begin{pmatrix} \psi_1 \cos \theta & 0 & \psi_2 \sin \theta \\ 0 & \psi_1 \cos \theta & 0 \\ \psi_2 \sin \theta & 0 & \psi_3 \cos \theta \end{pmatrix}, \quad (7)$$

where

$$\psi_1 = \frac{1}{\Omega^{*4}} \left[6 + \Omega^{*2} - \frac{6 + 3\Omega^{*2} - \Omega^{*4}}{\Omega^*} \arctan \Omega^* \right], \quad (8)$$

$$\psi_2 = \frac{6}{\Omega^{*4}} \left[3 - \frac{3 + \Omega^{*2}}{\Omega^*} \arctan \Omega^* \right], \quad (9)$$

$$\psi_3 = \frac{2}{\Omega^{*4}} \left[\frac{6 + 7\Omega^{*2}}{1 + \Omega^{*2}} - 3 \frac{\Omega^{*2} + 2}{\Omega^*} \arctan \Omega^* \right], \quad (10)$$

and $G = \sqrt{\mathbf{G}^2}$. θ is the colatitude, $\Omega^* = 2\tau_{\text{corr}}\Omega$ denotes the Coriolis number and τ_{corr} the convective turnover time of the stellar convection. Eq. (7) is valid for arbitrary rotation rate but weak fields. The zz -component differs from the ss - and $\phi\phi$ -components by magnitude and sign. In the limit of slow rotation, $\Omega^* \ll 1$, (7) becomes

$$\alpha^\rho \approx \Omega^* G \tau_{\text{corr}} u_t^2 \begin{pmatrix} \frac{4}{5} \cos \theta & 0 & -\frac{8}{5} \sin \theta \\ 0 & \frac{4}{5} \cos \theta & 0 \\ -\frac{8}{5} \sin \theta & 0 & -\frac{12}{5} \cos \theta \end{pmatrix}. \quad (11)$$

In the more relevant opposite limit of rapid rotation, $\Omega^* \gg 1$, the α -effect assumes the form

$$\alpha^\rho \approx G \tau_{\text{corr}} u_t^2 \frac{\pi}{2} \cos \theta \begin{pmatrix} 1 & 0 & 0 \\ 0 & 1 & 0 \\ 0 & 0 & 0 \end{pmatrix}. \quad (12)$$

In the latter case the tensor becomes two-dimensional. Note that in (12) the Coriolis number does not appear anymore, i.e. the α -effect becomes independent of the rotation rate.

Eq. (7) holds for arbitrary rotation rates but only weak fields. For finite field strengths, the back reaction on the small-scale motions reduces the α -effect and finally saturate the growth of the field at a value of the order of magnitude of the equipartition value. A calculation of this α -quenching process has been done by Rüdiger & Kitchatinov (1993) for the slowly rotating case. As this does not apply in our case, we adopt the simple and widely used expression

$$\alpha = \frac{\alpha_0}{1 + \beta^2}, \quad (13)$$

where $\beta = \sqrt{\langle \mathbf{B}^2 \rangle} / B_{\text{eq}}$ and $B_{\text{eq}} = \sqrt{\mu_0 \rho u_t^2}$ is the equipartition value for the magnetic field.

2.1.2. Diffusion

The diffusion is due to the simple presence of the turbulence. It does not depend on a gradient but on the length and time scales of the velocity fluctuations and on the rotation rate (Kitchatinov et al. 1994),

$$\eta_{ijk} = \eta_0 (\phi_1 + \phi_2) \epsilon_{ijk} + \eta_0 (\phi_1 - \phi_2) \epsilon_{ijl} \frac{\Omega_l \Omega_k}{\Omega^2}, \quad (14)$$

with $\eta_0 = \tau_{\text{corr}} u_t^2 / 3$ and

$$\phi_1 = \frac{3}{4\Omega^{*2}} \left(-1 + \frac{\Omega^{*2} + 1}{\Omega^*} \arctan \Omega^* \right), \quad (15)$$

$$\phi_2 = \frac{3}{2\Omega^{*2}} \left(1 - \frac{\arctan \Omega^*}{\Omega^*} \right). \quad (16)$$

For slow rotation, $\Omega^* \ll 1$, $\phi_1 \approx \phi_2 \approx 1/2$ and the diffusivity tensor becomes isotropic. For rapid rotation,

$$\phi_1 \approx \frac{3\pi}{8\Omega^*}, \quad \phi_2 \approx \frac{3}{2\Omega^{*2}}, \quad (17)$$

and the diffusivity tensor not only becomes strongly anisotropic, the diffusion being twice as effective along the z -axis than perpendicular to it.

For fast rotators, the α -effect ceases to grow with the rotation rate and saturates at a finite value. The diffusion term *decreases* like $1/\Omega^*$. The faster the star rotates, the more efficient (becomes) the dynamo process.

2.1.3. Turbulent transport

Besides the field-generating α -effect which is odd in the rotation rate, the density stratification also causes a pure transport effect which is even in the rotation rate, i.e.

$$\mathcal{E}_{\text{adv}} = \mathcal{E}_{\text{dens}} + \mathcal{E}_{\text{mag}}, \quad (18)$$

with

$$\mathcal{E}_{\text{dens}} = \mathbf{u}_{\text{dens}} \times \langle \mathbf{B} \rangle - \frac{2}{\Omega^2} (\mathbf{u}_{\text{dens}} \times \Omega) (\Omega \cdot \langle \mathbf{B} \rangle), \quad (19)$$

$$\mathcal{E}_{\text{mag}} = \mathbf{u}_{\text{mag}} \times \langle \mathbf{B} \rangle + \frac{1}{\Omega^2} (\hat{\mathbf{u}}_{\text{mag}} \times \Omega) (\Omega \cdot \langle \mathbf{B} \rangle), \quad (20)$$

where

$$\mathbf{u}_{\text{dens}} = -\mathbf{G}_{\perp} \tau_{\text{corr}} u_t^2 \chi_1(\Omega^*), \quad (21)$$

$$\mathbf{u}_{\text{mag}} = \mathbf{G} \tau_{\text{corr}} u_t^2 \chi_2(\Omega^*), \quad (22)$$

$$\hat{\mathbf{u}}_{\text{mag}} = -\mathbf{G}_{\perp} \tau_{\text{corr}} u_t^2 \chi_3(\Omega^*), \quad (23)$$

and

$$\mathbf{G}_{\perp} = \mathbf{G} - \Omega(\mathbf{G} \cdot \Omega)/\Omega^2. \quad (24)$$

In the limit of slow rotation, $\Omega^* \ll 1$,

$$\chi_1 \approx \frac{1}{15} \Omega^{*2}, \quad \chi_2 \approx \frac{1}{6} - \frac{1}{15} \Omega^{*2}, \quad \chi_3 \approx \frac{2}{15} \Omega^{*2}, \quad (25)$$

while in the opposite limit of rapid rotation, $\chi_1 \approx \pi/8\Omega^*$, $\chi_2 \approx \pi/16\Omega^*$, $\chi_3 \approx \pi/16\Omega^*$ (Kitchatinov 1991). This effect has been included for completeness, but is of minor importance in this context. For comparison, some runs were performed twice, once with and once without the transport effect. The results did not show any significant difference.

2.2. The star

In our computations constant values for the local parameters are used, which are taken from a model of a fully convective pre main-sequence star with 1.5 solar masses and 4.6 solar radii by Palla & Stahler (1993). Figure 1 shows the stratifications of density, equipartition field strength, convection velocity and convective turnover time. The convection velocity after

$$u_t = \left(\frac{L g l_{\text{corr}}^2 \Omega}{\pi^2 r^2 \rho C_p T} \right)^{\frac{1}{4}} \quad (26)$$

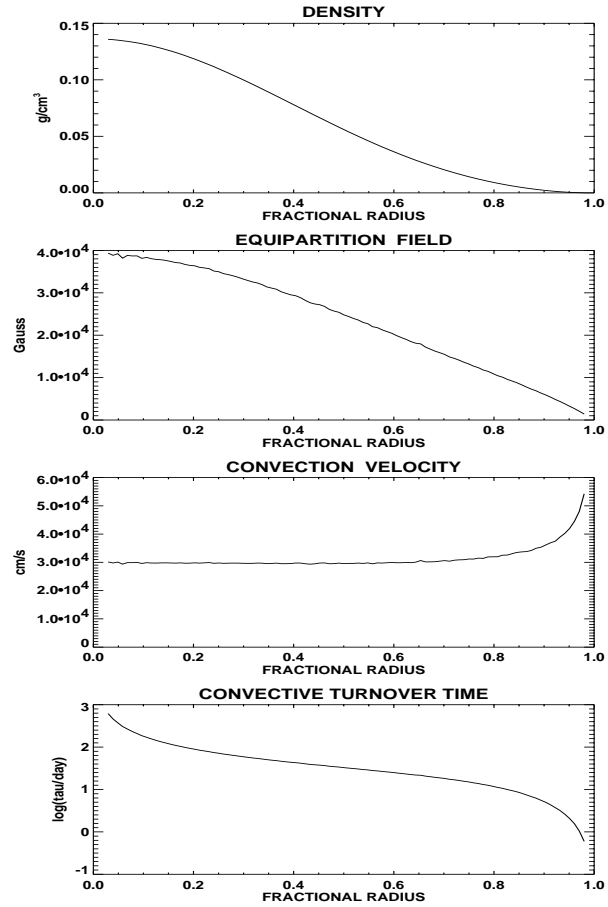


Fig. 1. The stratification of the T Tauri star: density, equipartition field strength, convection velocity, and logarithm of the convective turnover time in days (top to bottom)

(L luminosity, l_{corr} mixing-length) differs from that of standard mixing-length theory. It has been corrected to take into account the influence of the Coriolis force on the convective heat transport (Küker & Rüdiger 1997). A more consistent approach would be the use of rotation-dependent stellar models, i.e. to take into account the influence of the rotation in the stellar structure calculations, which is, however, beyond the scope of this paper. The corrected convection velocity is constant in the whole star except close to the surface. We use $\eta_0 = 10^{15}$ cm²/s for the turbulent magnetic diffusivity of the non-rotating star, 25 kG for the equipartition value of the magnetic field, and $G = -5$ for the density stratification. Note that the actual magnitude of the magnetic diffusivity depends on the rotation rate via the Coriolis number. A rotation frequency $\Omega = 10^{-5}$ s⁻¹ corresponding to a rotation period of about a week yields a Coriolis number $\Omega^* = 60$. This value is varied in some of the calculations below.

2.3. Numerics

As non-axisymmetric field configurations must be expected, a 3D code is necessary to solve the induction equation. We use the explicit time-dependent second-order finite-difference

scheme in three spatial dimensions by Elstner et al. (1990). The code uses cylindrical polar coordinates and a staggered grid representation of the EMF to ensure that the magnetic field remains divergence-free throughout the whole computation. While the use of cylindrical coordinates has the advantage of avoiding the singularity at the origin of the coordinate system, it does not allow detailed radial profiles of density, magnetic diffusivity and other relevant parameters. We use averaged values for these quantities as well as for their gradients where necessary. Moreover, it is not very convenient to impose any boundary conditions on the stellar surface. Instead, we assume the star to be surrounded by a corotating medium of large yet finite resistivity. This configuration is a good approximation of a vacuum boundary condition as test calculations confirmed (see below).

First we tried to reproduce results of Moss & Brandenburg (1995, MB), who studied an α^2 -type dynamo in a conducting sphere surrounded by vacuum. We used the same EMF inside the sphere while the value of the magnetic diffusivity outside the sphere was assumed ten times the inside. With a resolution of $61 \times 31 \times 9$ grid points, we varied the Coriolis number to determine the critical value. We find dynamo action for Coriolis numbers larger than about 26, a value slightly smaller than that of 27.9 found by MB. The linear mode that is most easily excited is the S1-mode, which also is the dominant one in the nonlinear case. Hence, we find the same geometry as MB, although the critical values for the Coriolis number slightly differ.

We did not make any attempts to improve the agreement between the models as it would have been very difficult to use the same boundary conditions as MB.

3. Results

We first address the question under which conditions dynamo action exists. We therefore fix the Coriolis number at a value of 60 and vary c_α from zero to one. The critical value for the onset of dynamo action lies close to 0.02. For all values of c_α above 0.02, the field has a S1-type geometry, i.e. the radial and azimuthal components are symmetric with respect to the equatorial plane while the z -component is antisymmetric, and all components vary with the azimuthal angle like $\cos(\phi + \omega t)$. The field has thus an approximately dipolar geometry, but with the axis of symmetry inclined by 90° relative to the rotation axis. The field rotates with the star with a slow drift with a period of about 45 years between both rotations. Figures 2 and 4 show the field geometry for $c_\alpha = 0.2$, $\Omega^* = 60$.

In the top diagram of Fig. 3, the total magnetic energy is plotted vs. the α -parameter. The plot clearly shows that above the critical value the energy increases linearly for increasing values of c_α . This behavior is not surprising since for a steady field the diffusion must balance the α -effect.

As we always find essentially the same field structure and $\alpha \propto 1/\beta^2$ for $\beta \gg 1$, the field energy must be a linear function of α_0 , hence of c_α .

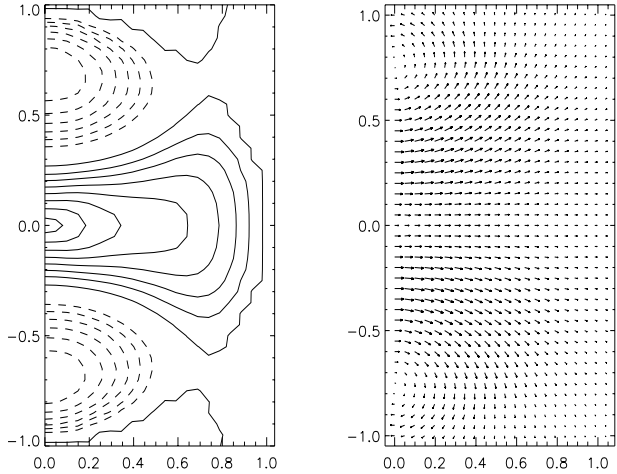


Fig. 2. Magnetic field for $\Omega^* = 60$ and $c_\alpha = 0.2$ in the $\phi = 0$ half-plane. LEFT: isocontours of the azimuthal (ϕ) component. RIGHT: vector plot of the radial and z -components

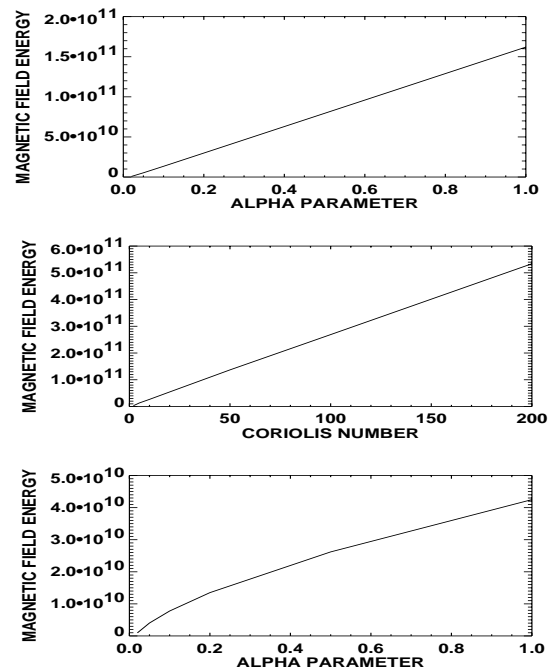


Fig. 3. TOP: Total magnetic energy in arbitrary units as a function of the dimensionless parameter c_α . MIDDLE: Total magnetic energy as a function of the Coriolis number. BOTTOM: Same as top but with different α -quenching law

Varying c_α means keeping the rotation rate constant while changing the efficiency of the α -effect. A more interesting case is that of constant c_α and varying Coriolis number, a situation which may indeed occur when a star spins down after reaching the main-sequence. We have carried out a sequence of runs with $c_\alpha = 1$ and increasing Coriolis number.

The critical value of Ω^* lies between 0.7 and 0.8. At $\Omega^* = 0.8$, we find a stationary field of S0 geometry, i.e. the field is

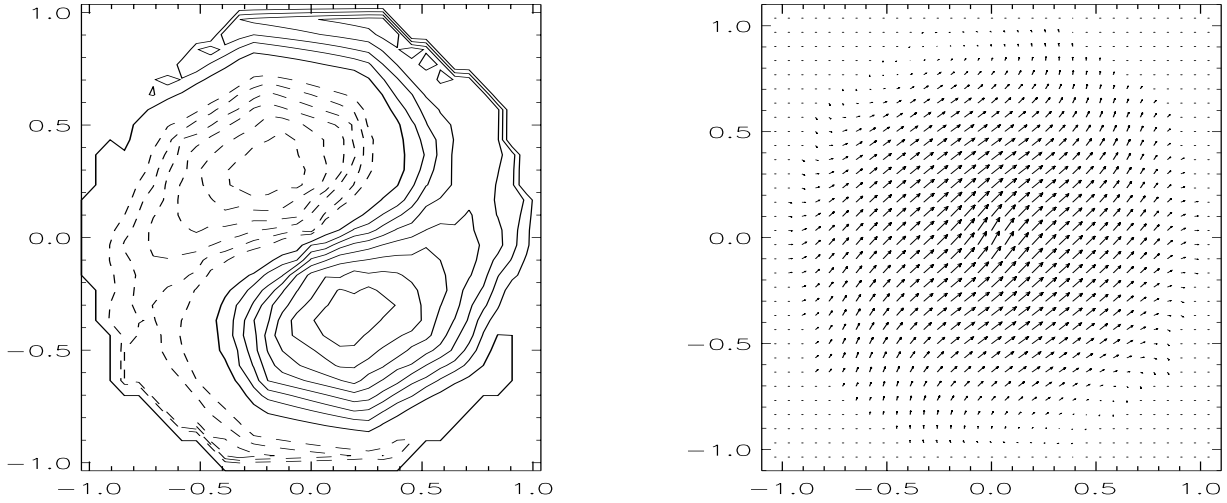


Fig. 4. The magnetic field in a plane of constant z . LEFT: isocontour plot of the z -component. RIGHT: vector plot of the horizontal components

symmetric with respect to the equator and it is axisymmetric. Figures 5 and 7 show the field structure.

At $\Omega^* = 1$, the field geometry has not changed very much, but the field is now oscillatory with an oscillation period of about two years. Its time dependence can not be described as a rotation, but is a true cycle with the total field energy varying with time. The same behavior as for $\Omega^* = 1$ is found at $\Omega^* = 2$.

For $\Omega^* = 3$ and all larger values, the field has S1-type geometry and a purely rotational time dependence with no variation of the magnetic field energy. The field geometry is shown in Figs. 6 and 8. In the s - ϕ plane, it is of almost spiral-type while a plot at constant azimuthal angle shows two radial shells. Above $\Omega^* = 3$, the field geometry does not change that much, although the profiles at constant z -values show a more spiral-type geometry for $\Omega^* = 3$ and an almost dipolar field for $\Omega^* = 60$.

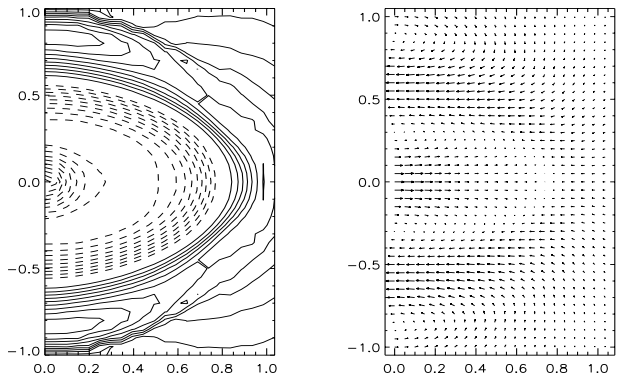


Fig. 6. Magnetic field for $\Omega^* = 3$ in the half-plane $\phi = 0$. LEFT: isocontours of the ϕ -component. RIGHT: the radial and vertical components

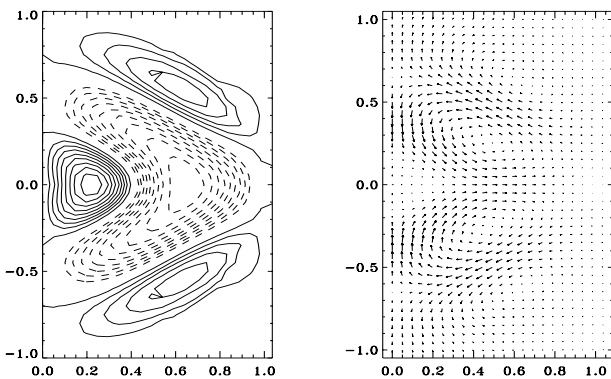


Fig. 5. Magnetic field for the weakly supercritical case $\Omega^* = 0.8$. LEFT: isocontours of the toroidal field. RIGHT: vector plot of the poloidal field

Changes of Ω^* affect both α and η , but in the limit of fast rotation, α_0 becomes independent of Ω^* , while the magnetic

diffusivity decreases as $1/\Omega^*$. Hence, $\beta^2 \propto \Omega^*$ and the magnetic field energy increases linearly with increasing Coriolis number. The result is shown in Fig. 3. The relation between Ω^* and the resulting magnetic field energy is indeed linear.

The linear relation between the field energy and c_α (or the Coriolis number) is a consequence of the α -quenching relation (13). In Rüdiger & Kitchatinov (1993), a quenching function was derived which decreases with β^3 in the limit of strong magnetic fields. We therefore vary c_α for fixed Coriolis number with $\alpha = \alpha_0/(1 + \beta^3)$. The result is shown in the bottom diagram of Fig. 3. Now $\beta^3 \propto \alpha_0$ and thus the magnetic energy varies as $\alpha_0^{2/3}$. The symmetry of the field is not affected by the change of the α -quenching function.

4. Conclusions

We never find the traditional dipolar field geometry. The fields are always symmetric with respect to the equatorial plane.

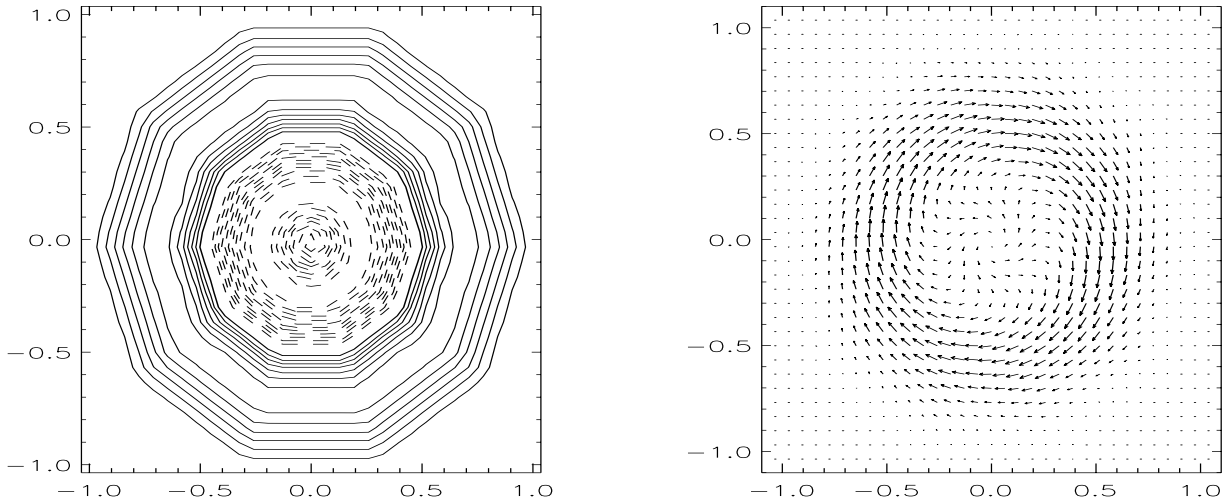


Fig. 7. The magnetic field for $\Omega^* = 0.8$ in a plane of constant z somewhere above the equatorial plane. LEFT: isocontour plot of the z -component. RIGHT: vector plot of the horizontal components

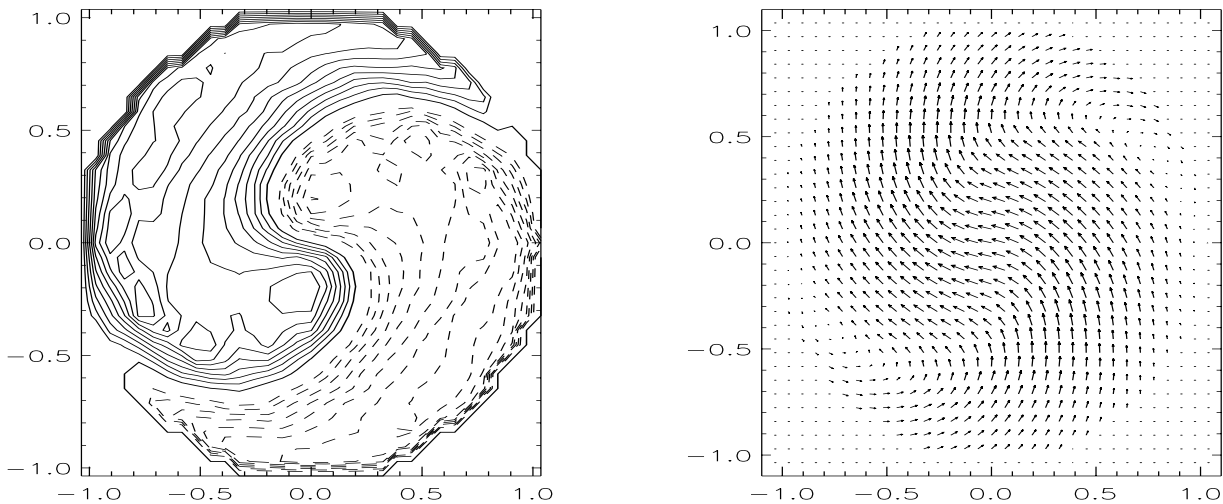


Fig. 8. Same as Fig. 7, but for $\Omega^* = 3$

Small Coriolis numbers yield axisymmetric (S0) and large Coriolis numbers non-axisymmetric (S1) field geometries. While the S0-field consists of quadrupolar and higher modes with no dipolar contribution at all, the non-axisymmetric field found for realistic Coriolis numbers somewhat resembles a tilted dipole. Note, however, that it remains fully three-dimensional in the outer space, while an aligned dipole has no toroidal field component. For the stellar model we have used, a Coriolis number of order 2 would correspond to a rotation period of 220 days, much longer than the observed rotation periods of up to one week. We therefore conclude that the mean magnetic fields in weak-line T Tauri stars are non-axisymmetric.

It is a well-known result of linear dynamo theory, that non-axisymmetric modes can merely rotate, not oscillate (Rädler

1986). Although we deal with nonlinear dynamos, this is exactly the behavior we find. The fields are time-dependent, but their variation turns out to be a pure rotation.

The field geometry that results from our model is quite close to what MB found, although we deal with a different kind of object and a completely different α -tensor. This is due to the fact that α^2 -type dynamos do not depend on the sign of α . Moreover, both α -tensors have essentially the same form because the gradients of density and turbulence velocity are aligned (with opposite signs). Both types of α -effect share the property that α_{zz} vanishes for rapid rotation, while it dominates in case of slow rotation.

The field geometry appears not to depend significantly on the type of α -quenching used to limit the field generation. The field strength, however, does. While its order of magnitude is

determined by the equipartition field strength, the actual value depends on the input parameters c_α and Ω^* as well as on the quenching function. The field strength inside the star typically ranges between 10^4 and 10^5 G. Its dependence on the Coriolis number implies that even in a pure α^2 -type dynamo without any rotational shear, the magnetic field strength strongly depends on the stellar rotation rate.

The mechanism of field generation completely changes when the star contracts towards the main-sequence and the radiative core evolves. The strong rotational shear between the core and the convection zone should then turn the dynamo from the α^2 to the $\alpha\Omega$ -regime. It is a challenge for the theories of differential rotation and stellar dynamos to make predictions about this transition.

Acknowledgements. The authors are thankful for the support by the Deutsche Forschungsgemeinschaft. F. Palla is cordially acknowledged for his kind supply of current TTS models.

References

- Armitage P.J., Clarke C.J., 1996, MNRAS 280, 458
 Bouvier J., Cabrit S., Fernández M., et al., 1993, A&A 272, 176
 Camenzind M., 1990, Magnetized disk-winds and the origin of bipolar outflows. In: Klare, G. (ed.) Reviews in Modern Astronomy 3. Springer-Verlag, Berlin, p. 234
 Cameron A.C., Campbell C.G., 1993, A&A 274, 309
 Edwards S., Strom S.E., Hartigan P., et al., 1993, AJ 106, 372
 Elstner D., Meinel R., Rüdiger G., 1990, Geophys. Astrophys. Fluid Dyn. 50, 85
 Ghosh P., 1995, MNRAS 272, 763
 Hatzes A.P., 1995, ApJ 451, 784
 Johns-Krull C.M., Hatzes A.P., 1997, ApJ 487, 896
 Joncour I., Bertout C., Ménard F., 1994a, A&A 285, L25
 Joncour I., Bertout C., Bouvier J., 1994b, A&A 291, L19
 Kitchatinov L.L., 1991, A&A 243, 483
 Kitchatinov L.L., Pipin V.V., Rüdiger G., 1994, Astron. Nachr. 315, 157
 Königl A., 1991, ApJ 370, L39
 Krause F., Rädler K.H., 1980, Mean-Field Magnetohydrodynamics and Dynamo Theory. Akademie-Verlag, Berlin
 Krivodubskij V.N., Schultz M., 1993, Complete alpha-tensor for solar dynamo. In: Krause F., Rädler K.-H., Rüdiger G. (eds.) IAU Symp. 157, The cosmic dynamo. Kluwer, Dordrecht, p. 25
 Küker M., Rüdiger G., 1997, A&A 328, 253
 Li J., Wickramasinghe D.T., Rüdiger G., 1996, ApJ 469, 765
 Moss D., Brandenburg A., 1995, Geophys. Astrophys. Fluid Dyn. 80, 229 (MB)
 Palla F., Stahler S.W., 1993, ApJ 418, 414
 Parker E.N., 1993, ApJ 408, 707
 Rädler K.-H., 1986, Astron. Nachr. 307, 89
 Rice J.B., Strassmeier K.G., 1996, A&A 316, 164
 Rüdiger G., Elstner D., 1994, A&A 281, 46
 Rüdiger G., Kitchatinov L.L., 1993, A&A 269, 581
 Schüssler M., 1983, Stellar dynamo theory. In: Stenflo, J.O. (ed.) Proc. IAU Symp. 102, Solar and Stellar Magnetic Fields: Origins and Coronal Effects. D. Reidel, Dordrecht, p. 213
 Shu F., Najita J., Ostriker E., et al., 1994, ApJ 429, 781
 Wang Y.-M., 1995, ApJ 449, L153
 Yi I., 1994, ApJ 428, 760